



Composite calcite and opal test in Foraminifera (Rhizaria)

Julien Richirt¹, Satoshi Okada¹, Yoshiyuki Ishitani¹, Katsuyuki Uematsu², Akihiro Tame², Kaya Oda¹,
Noriyuki Isobe³, Toyoho Ishimura⁴, Masashi Tsuchiya⁵, Hidetaka Nomaki¹

¹ SUGAR, X-star, Japan Agency for Marine-Earth Science and Technology (JAMSTEC), 2-15 Natsushima-cho, Yokosuka
5 237-0061, Japan

² Marine Works Japan Ltd., 3-54-1 Oppamahigashi-cho, Yokosuka, Kanagawa, 237-0063, Japan

³ Research Institute for Marine Resources Utilization (MRU), Japan Agency for Marine-Earth Science and Technology
(JAMSTEC), Yokosuka, Kanagawa, 237-0061, Japan

⁴ Graduate School of Human and Environmental Studies, Kyoto University, Yoshidanihonmatsu, Sakyo-ku, Kyoto 606-8501,
10 Japan

⁵ Research Institute for Global Change (RIGC), Japan Agency for Marine-Earth Science and Technology (JAMSTEC),
Yokosuka, Kanagawa, 237-0061, Japan

Correspondence to: Julien Richirt (richirt.julien@gmail.com)

Abstract. Foraminifera are unicellular eukaryotes known to have a shell, called test, generally made of secreted calcite
15 (CaCO₃). We report for the first time a Foraminifera having a composite calcite/opal test in the cosmopolitan and well-studied
benthic species *Bolivina spissa* (Rotaliida), sampled from the Sagami Bay in Japan at 1410 m depth. Based on comprehensive
investigations including Scanning Electron Microscopy (SEM) coupled with Energy Dispersive X-ray Spectroscopy (EDS)
and Fourier Transform Infrared Spectroscopy (FTIR), we inspect the morphology and composition of the novel opaline layer
coating the inside part of the calcitic test. Using Scanning Transmission Electron Microscopy (STEM) and EDS analyses, we
20 detected probable Silica Deposition Vesicles (SDVs), organelles involved in opal precipitation in other silicifying organisms,
confirming that the Foraminifera themselves secrete the opal layer. The layer was systematically found in all studied individuals
and had no apparent sub-structure. Its thickness showed an analogous growth pattern with the calcitic shell of *B. spissa*, being
the thickest in the oldest chamber (proloculus) and becoming thinner toward the younger chambers (apertural side). Its absence
in the youngest chambers indicates that silicification occurs subsequently to calcification, probably discontinuously. We further
25 discuss the potential function(s) of this composite test and propose that the opal layer may serve as a protection barrier against
predators using either mechanical drilling or chemical etching of the calcitic test. Isotopic composition measurements
performed separately on the proloculus part and the apertural side of *B. spissa* suggest that the presence of an opal layer may
alter the calcitic isotopic signal and impact paleoenvironmental proxy using foraminifer's tests composition. If silicification in
Foraminifera was found to be more widespread than previously thought, it could possibly have important implications for
30 foraminiferal evolution, palaeoceanographic reconstructions, and the silica cycle at global scale.



1 Introduction

Silicon (Si) is the second most abundant element (27.2 wt. %) in the earth crust after oxygen (Greenwood and Earnshaw, 1997). In nature, silicon occurs generally in the form of silicate minerals (e.g., aluminosilicates) and silicon dioxide (SiO₂, e.g., quartz). Its soluble form, orthosilicic acid Si(OH)₄, is biologically assimilable, and biogenic silica, also referred to as biogenic opal (amorphous hydrated silica, SiO₂·nH₂O), is the second most abundant mineral type formed by organisms after carbonate minerals. A wide range of marine organisms such as sponges or protists, including diatoms, radiolarians or silicoflagellates (dictyochales), are able to take up Si(OH)₄ from their surrounding water and use silicon to build their shells or skeletons (Brümmer, 2003; Ehrlich et al., 2016). The silicified protistan shells were proposed to serve various and not mutually exclusive functions, such as defence against grazers, buoyancy, light modulation, catalysis of carbon assimilation, maintenance of shape and orientation or defence against viruses (Knoll & Kotrc, 2015).

Foraminifera (Rhizaria), belonging to the SAR group (i.e., Stramenopiles, Alveolata and Rhizaria, Burki et al., 2020), are one of the most widespread unicellular eukaryotes inhabiting both benthic and pelagic realms. They are characterised by the presence of a shell called “test” which can be organic, agglutinated (typically attaching sediment particles) or constituted of precipitated minerals (Sen Gupta, 2003). In the last category, almost all species precipitate calcium carbonate (CaCO₃). Having a high diversity with ~ 4000 recent living hard-shelled species able to fossilise (Murray, 2007), they show a profuse fossil record starting in the Cambrian (Culver, 1991). Consequently, the group is intensively employed for palaeoceanographic studies and palaeoenvironmental reconstructions (e.g., Murray, 2006, Jones, 2013), and geochemical measurements of their test have been extensively used to gain most of our knowledge on the past ocean responses to climate change (e.g., Katz et al., 2010). Additionally, Foraminifera play an important role in the global carbon cycle through remineralisation, especially in poorly oxygenated environments (Piña-Ochoa et al., 2010; Cesbron et al., 2016) and carbonate production (Langer, 2008). Although exact calcification process is still in debate (de Nooijer et al., 2014; Toyofuku et al., 2017; Nagai et al., 2018; Ujjié et al., 2023), different foraminiferal sub-orders are known to exhibit different test structure organisations (Hansen, 2003) and geochemical compositions (de Nooijer et al., 2023).

While silica precipitation occurs frequently in most of lineages of the SAR group (Marron et al., 2016), it was only very rarely described in Foraminifera. The first report was made by Brady in late 19th century, who wrote that the test of some benthic foraminifera assigned to *Miliolina* from the abyssal area of North Pacific was not dissolved by acid, and that their usual calcareous shell was totally or partially replaced by a thin siliceous investment, which exhibited a perfectly homogeneous texture (p. xvii, Brady, 1884). However, no supplementary information about this observation is available and these specimens might have been agglutinating foraminifera having a very smooth test. Almost one century later, Echols (1971) reported rare individuals of ‘*Miliolinella*’ sp. presenting a wall insoluble in dilute hydrochloric acid, lacking apparent agglutinated particle, and possibly composed of opaline silica in sediment sampled at various depths (990–4640 m water depth) in the Scotia Sea, Southern Ocean. A benthic foraminiferal species sampled in the Indian Ocean at depth ranging from 5266–5420 m was also described as having an opaline shell, because it was insoluble in hydrochloric acid (*Miliammellus legis*, Saidova &



Burmistrova, 1978). This species, being the only representant in the newly established genus *Miliammellus*, was placed into
65 the order Miliolida because of its general morphology (Burmistrova, 1978). However, Lipps already argued in 1973 that
insolubility in acids is not a conclusive experiment, because an organic cement would hold the test together such as in
specimens assigned to Rzehakinidae (Cushman, 1933), introducing foraminifera having a “siliceous or agglutinated” wall that
disaggregate in hydrogen peroxide but resist acid dissolution. Additionally, in the case of fossil species that do not disaggregate
in hydrogen peroxide, taphonomic processes might have stabilised the organic matter cement, making this test inconclusive
70 for fossilised specimens. In 1980, Resig et al. described a species sampled from the Pacific Ocean at ~ 4400 m depth as
presenting an imperforate test uniquely constituted of silica (*Silicoloculina profunda*, Resig, Lowenstam, Echols & Weiner,
1980), and created a new suborder (*Silicoloculinina*) based on the wall construction type (imperforate test made of secreted
opaline silica). The authors imaged the fine structures of the test and investigated its composition, validating its opaline silica
nature, and concluding that the test was secreted by the Foraminifera. The remarkable similarity regarding the descriptions
75 given in Burmistrova (1978) and Resig et al. (1980) led to the conclusion that they certainly described the same species, making
Silicoloculina profunda a junior synonym of *Miliammellus legis* (as referenced in WoRMS database). The presence of silicate
grains within the calcitic test was reported in *Melonis baarleanus* (Rotaliida) but were supposed to be from a sedimentary
origin (Borrelli et al., 2018). While biosilicification have commonly been reported in other rhizarian groups such as radiolarians
or cercozoans (Marron et al., 2016; Hendry et al., 2018), only scarce observations of foraminifers having a silica test were
80 reported and their silica mineralisation process is totally unknown. To date, *M. legis* (Miliolida) is the only species reported as
having a secreted siliceous test for this group.

Here we report the systematic presence of an opaline layer in the test in the cosmopolitan benthic species *Bolivina spissa*
(Rotaliida) sampled at 1410 m depth in the Sagami Bay (Japan). The composite test is composed of two different materials:
an external calcitic test, typical from hyaline and porcelaneous Foraminifera, and an internal layer composed of biogenic silica
85 (opal) coating the inside part of the calcitic test. Different observational and measurement methods were used to describe the
composition, morphology and presumed precipitation mechanism of this opal layer, including Scanning Electron Microscopy
(SEM), Transmission Electron Microscopy (TEM), Energy-Dispersive X-ray Spectroscopy (EDS) and Fourier-Transform
Infrared spectroscopy (FTIR). Based on these comprehensive observations, we further discuss the potential function(s) of this
composite test, its potential impact on paleoenvironmental reconstructions using foraminifer’s tests composition and its
90 possible importance for biogeochemical cycles understanding.

2 Material & Methods

2.1 Sampling sites

Sediment cores were collected using the research deep submergence vehicle (DSV) *Shinkai 6500* on-board R/V *Yokosuka*, in
the central part of the Sagami Bay (NSB site, 35°00.3' N 139°22.7' E) at 1410 m depth (Fig. 1), during three sampling
95 campaigns in May 2022 and 2023, and October 2022 (Table 1).

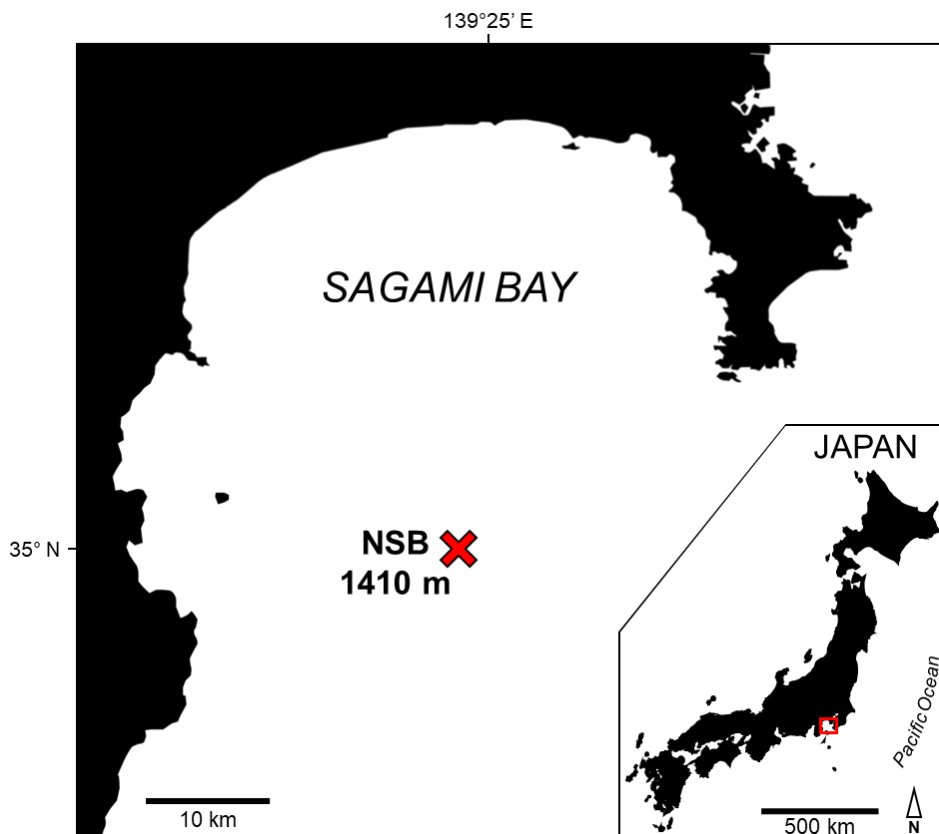


Figure 1: map of Japan (bottom right panel) indicating the localisation of the Sagami Bay (main panel). Sampling site NSB (red cross) and sampling depth are indicated.

100 Table 1 resumes the samples origin and the type of analyses performed. *Bolivina spissa* specimens were isolated from different sediment depth interval (topmost cm or down to 5 cm depth) under a stereomicroscope and were fixed using different technics (cryo-fixed on board: Okada et al. submitted, frozen at -80°C , glutaraldehyde fixed, or air dried).

Table 1: Sampling period, sediment interval, type of analyse, fixation type and timing and number of specimens analysed in this study.

Sampling period	Sediment interval	Type of analyse	Fixation type	Fixation timing	Number of specimens analysed
May 2022	0-1 cm	Cryo-SEM and EDS	Cryo-fixed	Isolated ~1.5 months after sampling from a bucket of sediment stored in the lab at 4°C	1
October 2022	0-1 cm	Cryo-SEM and EDS	Cryo-fixed	Cryo-fixed directly on board after sampling	6
May 2022	0-1 cm and 1-5 cm	Environmental SEM	Frozen at -80°C	Sample frozen -80°C directly on board after sampling	15
May 2022	every cm from 0-1 cm to 3-4 cm	TEM and EDS	Glutaraldehyde 4%	Fixed directly on board after sampling	8
May 2023	0-2 cm	FTIR spectroscopy	Air dried	Isolated ~3 months after sampling from a bucket of sediment stored in the lab at 4°C	3
October 2022	0-5 cm	Isotopic composition of calcite	Air-dried	Isolated ~2 months after sampling from a bucket of sediment stored in the lab at 4°C	17



2.2 Cryo-SEM imaging & EDS mapping

105 After live checks (based on the presence of sediment aggregation at the aperture and cytoplasm coloration), isolated living
specimens were processed following the protocol described in Okada et al. (submitted). Briefly, specimens were embedded in
a sucrose-based or glycerol-based aqueous glue, cryofixed (in liquid nitrogen-cooled isopentane) and stored at c.a. -170°C .
Cross-section of the specimens were exposed using a diamond knife in a cryo-ultramicrotome, aiming for a clean cut to
eliminate topographic variations of the sample surface. Scanning electron microscope (SEM) observation was performed on a
110 Helios G4 UX (Thermo Fisher Scientific) equipped with gallium focused ion beam (FIB) gun, an energy dispersive X-ray
spectroscopy (EDS) detector (Octane Elite Super C5, AMETEK), and a cryogenic stage with a preparation chamber (PP3010T,
Quorum). After sublimation of overlying water ice (~ 5 min at $\sim -80^{\circ}\text{C}$), several SEM images in backscattered electron mode
were acquired and aggregated to obtain a high-resolution SEM image for all individuals ($n = 7$). The elemental composition
was then mapped by EDS analysis without conductive coating of the sample to avoid possible overlaps of EDS peaks of the
115 coating metals.

After spectra treatment to deconvolve signal from noise (correction for the bremsstrahlung effect, Supplementary Method 1),
the colocalisation of SEM images and EDS elemental maps were done manually using calcium distribution maps (Ca EDS),
the main compound of the test in calcitic foraminifera (SEM images). EDS maps scaling and/or rotation were performed when
necessary but deformation (i.e., warping) was never applied. Finally, to obtain a Si mapping from non-sedimentary origin,
120 aluminium (Al) signal was subtracted to the silicon (Si) signal to remove aluminosilicate particles (typical from clay minerals,
major compound of the sediment at the sampling site) from EDS maps.

Additionally, the thickness of the Si layer was measured in each separate chamber (numbered from the proloculus toward the
apertural side) on all available specimens.

Image treatments and measurements were done using the software Fiji (Schindelin et al., 2012).

125 2.3 Low-vacuum SEM imaging

To expose the Si layer below the calcitic test, isolated and air-dried individuals ($n = 15$) were subsequently immersed in 0.5
M ethylene-diamine-tetraacetic acid disodium salt solution (EDTA, 03690 - Sigma Aldrich) for 48 h and then rinsed with
distilled water before observation. After, specimens were put on an aluminium stub on carbon tape prior observation with a
benchtop SEM (JEOL JCM-6000Plus) in low vacuum mode, without coating, at 15 kV of acceleration voltage and using
130 backscattered electron mode. In addition, optic pictures using a camera mounted on a stereomicroscope were obtained both
before and after decalcification step.

2.4 TEM imaging & EDS measurements

To search for potential organelles involved in biosilicification, we observed the cytoplasm content using a transmission
electron microscope (TEM) and performed high-angle annular dark-field scanning transmission electron microscopy



135 (HAADF-STEM) coupled with EDS analyses. Directly on board, from different sediment layers of one cm thickness (0-1cm
to 4-5 cm depth), isolated and live checked specimens ($n = 8$) were fixed with glutaraldehyde. Specimens were then embedded
in 1 % aqueous agarose and cut into ~ 1 mm cubes. Samples were decalcified with 0.2 % ethylene glycol tetraacetic acid
(EGTA) in 0.81 mol L^{-1} aqueous sucrose solution (pH 7.0) for several days, rinsed with filtered seawater and postfixed with 2
140 with 1 % aqueous uranyl acetate for 2 h at room temperature. Stained samples were rinsed with milli-Q water, dehydrated in
a graded ethanol series, and embedded in epoxy resin. Blocs were further sectioned into ultra-thin sections (60 nm thick) which
were then placed on a formvar-supported copper grid mesh and subsequently stained with 2% aqueous uranyl acetate and lead
stain solution (0.3 % lead nitrate and 0.3 % lead acetate Sigma-Aldrich). TEM observations were done with a bottom-mounted
2k \times 2k Eagle charge-coupled device (CCD) camera (Tecnai G2 20, Thermo Fisher Scientific). Elemental compositions were
145 obtained by EDS analyses performed using an EDAX Genesis system under scanning electron microscopy (STEM) mode at
an acceleration voltage of 120 kV and 200 kV, respectively.

2.5 FTIR spectroscopy

The topmost 2 cm sediment from NSB station were sieved on a $63 \mu\text{m}$ mesh size sieve and *B. spissa* specimens were isolated
from the residue. Only specimens showing a completely empty shell and having a translucent aspect were selected to avoid the
150 presence of remaining cytoplasm in the test. To remove the calcitic layer and expose the underlying Si layer of the test, empty
tests were then immersed in 0.5 M EDTA (03690, Sigma Aldrich) for 24 h, rinsed with milli-Q water, placed on a calcium
fluoride (CaF_2) plate, and dried in a vacuum chamber prior measurement. Dried samples were measured using a microscope
infrared spectrometer (FTIR 6200 with IRT-7000, Jasco Inc.) with an aperture size of $15 \times 15 \mu\text{m}$. Transmission IR signals
were background-corrected to determine the infrared spectra between $4000\text{--}750 \text{ cm}^{-1}$ spectral region for a total of three
155 specimens. Because CaF_2 absorbs below 1000 cm^{-1} , no band assignments was done in this region (Mayerhöfer et al., 2020).

2.6 Isotopic analyses

In total, 17 specimens of *B. spissa* were isolated from NSB site sediment and micro-dissected in two parts using a scalpel
aiming to separate the oldest part (proloculus side) from the newest part of the test (apertural side). Because it was challenging
to dissect only the proloculus from the other chambers on the apertural side, few chambers were still attached to the proloculus
160 prior measurements (6 microspheric and 11 macrospherics individuals, Supplementary Fig. 1). Stable carbon and oxygen
isotopic compositions ($\delta^{13}\text{C}$ and $\delta^{18}\text{O}$, respectively) of dissected parts were determined using a high precision microscale
carbonate isotopic analytical system, MICAL3c (Ishimura et al., 2004; 2008). Samples were reacted with H_3PO_4 to produce
 CO_2 . After purification, CO_2 was introduced into an IsoPrime100 isotope ratio mass spectrometer (IsoPrime Ltd., Cheadle
Hulme, UK) equipped with a customized continuous-flow gas preparation system (MICAL3c) at Kyoto University. This
165 system allows us to determine the $\delta^{13}\text{C}$ and $\delta^{18}\text{O}$ values of as little as $0.1 \mu\text{g CaCO}_3$ with an analytical precision of better than



± 0.10 ‰. The isotopic values were standardised to the Vienna Pee Dee Belemnite (VPDB) scale and expressed in δ notation. The mass of dissected samples was estimated from the volume of CO_2 gas produced during the reaction between CaCO_3 and H_3PO_4 .

3 Results

170 3.1 Morphology of the silicon coating the inside part of the calcitic test

Macrospheric (haploidic) and microspheric (diploidic) specimens were observed with a stereomicroscope (Fig. 2a & 2d) before being imaged in low-vacuum SEM settings (Fig. 2b & 2e). Specimens showed a costate proloculus, acute carinate edges and sometimes a minute apical spike, typical from the morphospecies *Bolivina spissa*. The same specimens were then imaged again in low-vacuum SEM settings (Fig. 2c & 2f) after the dissolution of their calcitic shell to expose the underlying Si layer.

175 In all individuals, the last few newer chambers were always missing and/or collapsed after decalcification, while the older chambers on the proloculus side remained well shaped (Fig. 2c & 2f).

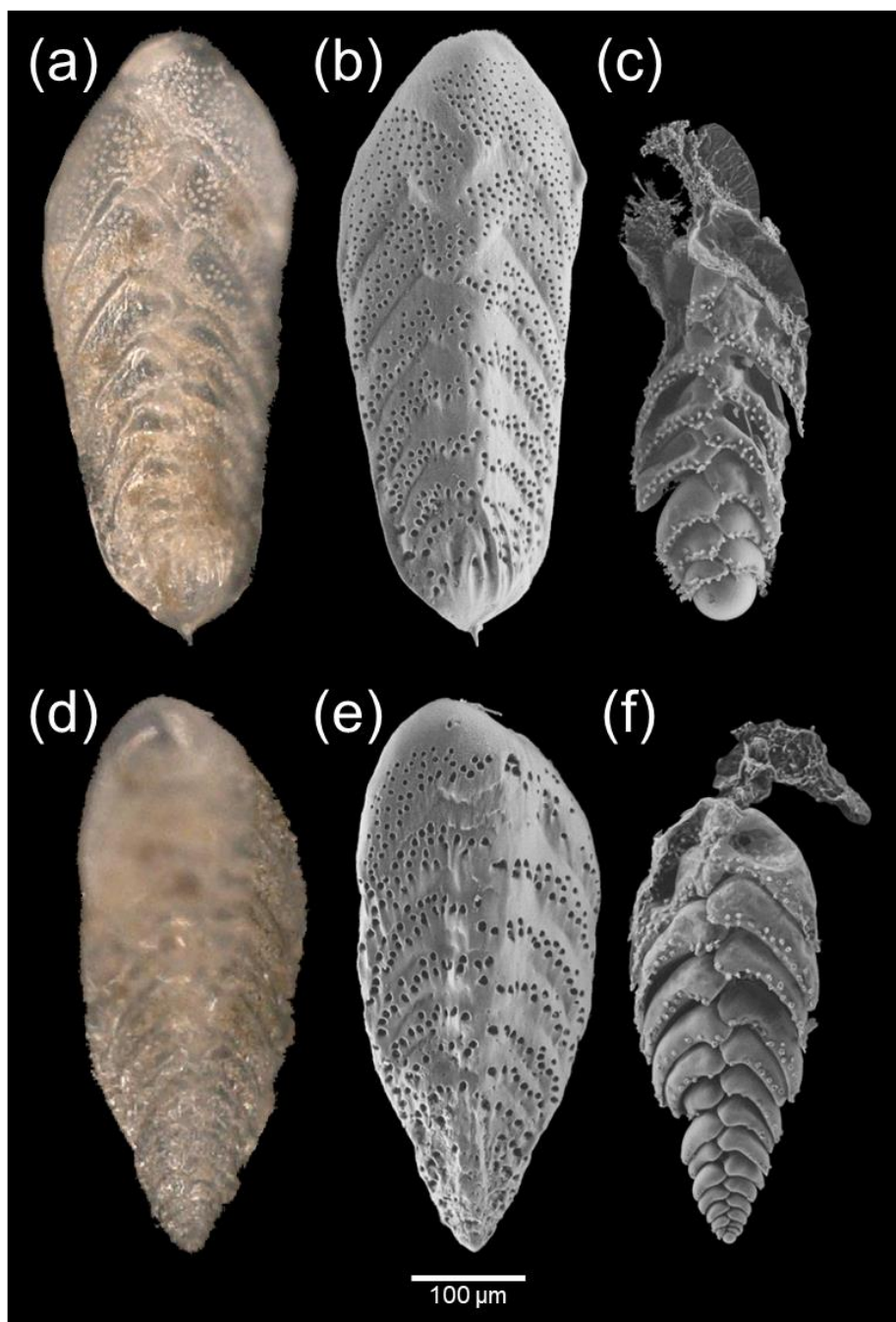


Figure 2: Macrospheric (a–c) and microspheric (d–f) *Bolivina spissa* specimens, imaged with stereomicroscope (a and d) and low-vacuum SEM before (b and e) and after (c and f) decalcification to expose the Si layer below the calcitic shell.

180 Figure 3a shows the Si layer connexions between consecutive chambers. Funnel-like structures were visibly sticking out at the pore's location after decalcification, coating the inner surface of the original pore's calcitic wall (Fig. 3b). These funnel-like

structures were not made of Si but were probable remains of organic material, the Si internal coating being visibly terminated at the pore plate from cryo-SEM (Fig. 3c) and TEM observations (Supplementary Fig. 2 & 3). The texture of the Si layer's surface always appeared smooth without visible substructures (excluding where pores priorly occurred), and the proloculus was nearly spherical (Fig. 3d).

185

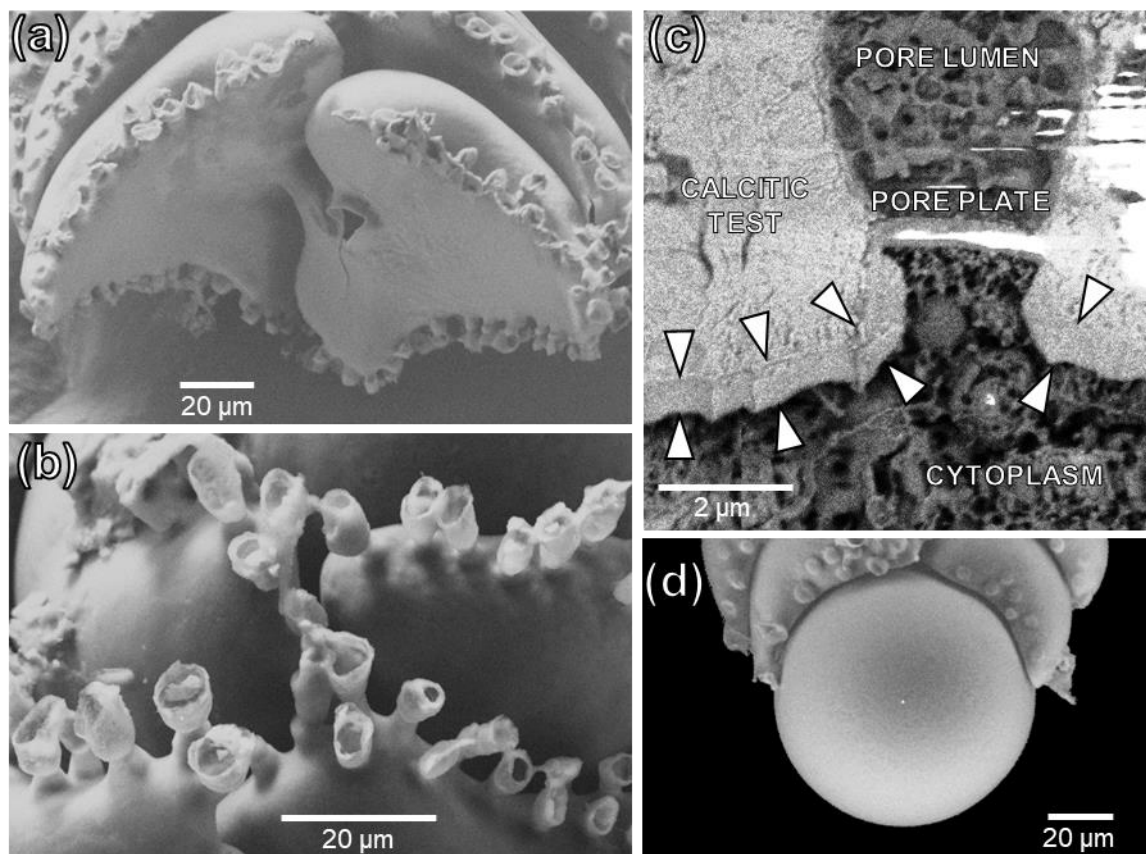
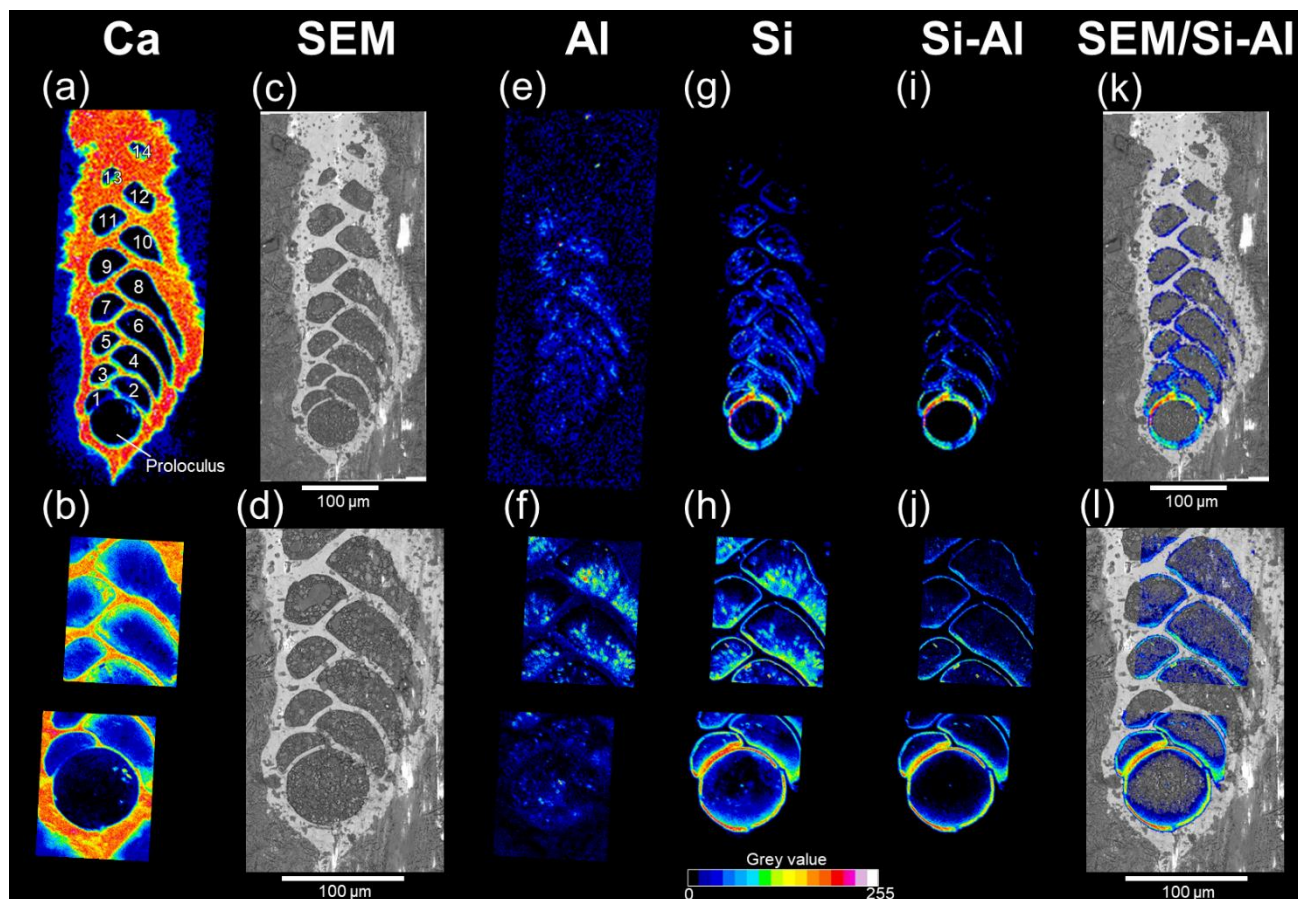


Figure 3: SEM images of the silicified structures of *B. spissa*. (a) Broken *B. spissa* after decalcification to expose the Si layer connexions between successive chambers. (b) Magnification on the pore funnel-like structures of *B. spissa* exposed after decalcification. (c) Transversal section of a pore imaged with cryo-SEM on non-decalcified *B. spissa*. White arrows indicate the position of the Si layer. White colour on the top right of the image and on the pore plate is due to overcharging. (d) Magnification of the proloculus of *B. spissa* exposed after decalcification.

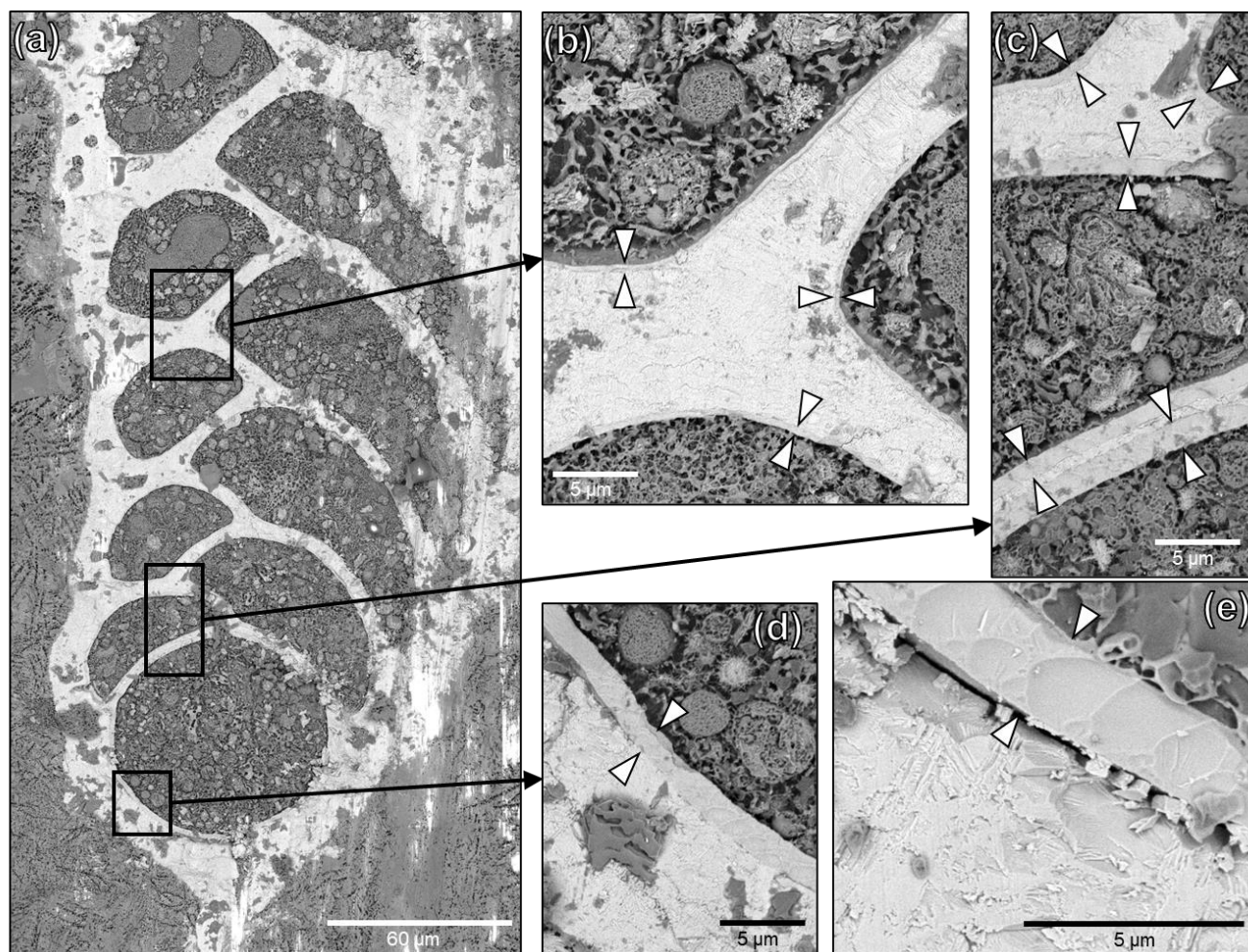
190

Figure 4 illustrates the different steps performed to obtain the Si distribution maps from non-sedimentary origin which was finally superimposed on the cryo-SEM images. The calcium distribution followed the electron-dense area SEM images representing the calcitic test of individuals (Fig. 4a–d). Sedimentary aluminosilicate was removed by subtracting aluminium signal from that of silicon (Fig. 4e–j), and the resulting signal showed that the silicon was localised on the inner wall of the calcite test (Fig. 4k–l). The Si lining from non-sedimentary origin was systematically found in all the seven specimens analysed (Table 1) and the signal was always stronger in the older chambers (proloculus side) than in the newer chambers (aperture side, Fig. 4i–2l).

195



- 200 **Figure 4:** SEM imaging and EDS maps (16 colours grey value scale) of a representative cryo-fixed *B. spissa* (a, c, e, g, i and k) and magnification on areas of interest (b, d, f, h, j and l). (a and b) EDS maps of Ca used to colocalise EDS elemental maps and SEM images. Proloculus is indicated and chambers are numbered. (c and d) SEM images of a cryo-cracked specimen. (e and f) EDS maps of Al. (g and h) EDS maps of Si. (i and j) Resulting EDS maps from the subtraction of the Al signal to Si signal (i.e., removing aluminosilicate). (k and l) Superimposition of Si map from non-sedimentary origin over SEM images.
- 205 The Si layer was clearly identifiable on cryo-SEM images as a less electron-dense structure coating the internal part of the calcitic test (Fig. 5). The thickness of this Si layer was constant inside individual chamber for a given specimen. The decreasing Si signal from proloculus toward apertural side detected on EDS maps (Fig. 4i–l) was confirmed by observations on cryo-SEM images as visible decreasing thickness of the layer (Fig. 5). The Si layer was homogeneous without any visible layering even on the thickest sections and exhibited conchoidal fracture which is typical for glassy nature materials (Fig. 5e). No other visible
- 210 structure was observed between the Si layer structure the calcitic shell, which were in direct contact. In very rare cases, we observed a hollow part between the two layers such as on Fig. 5e, that we ascribe to preparation artifact (i.e., cutting step).



215

Figure 5: Cryo-SEM images of representative cryo-cracked *B. spissa* specimen. (a) Overview of the specimen and (b–e) magnified regions of interest (black squares) to visualise the Si layer (indicated by white arrows) coating the inside part of the calcitic test. Note the decreasing thickness of the layer from the proloculus toward newer chambers. (e) magnified cryo-SEM image of the Si layer in a proloculus showing the homogeneity of the structure. Note the conchoidal fracture pattern typical from glassy nature material. The hollow part between the calcitic shell and the Si layer was very rarely observed and is resulting from the cutting step.

220

Thickness of the Si layer was equivalent considering each separate chamber and ranged from 1.65 to 0.05 μm , respectively measured in the proloculus part and in the last chamber of the individual where the Si layer was still visible (Supplementary Table 1). Data presented here must be considered carefully because a sub-perpendicular cracking orientation could introduce a bias in the actual thickness of the Si layer in each specimen. The Si layer was not visible in chambers newer than chamber 12 while the number of visible chambers was higher than 12 in five over seven specimens (Supplementary Table 1). However, the cryo-SEM image definition might have not been sufficient to detect structures smaller than 0.05 μm , corresponding to about four pixels in the acquired images. Thickness data indicated that the decreasing trend in the Si layer thickness follows an inverse power law ($r^2=0.99$, Fig. 6).

225

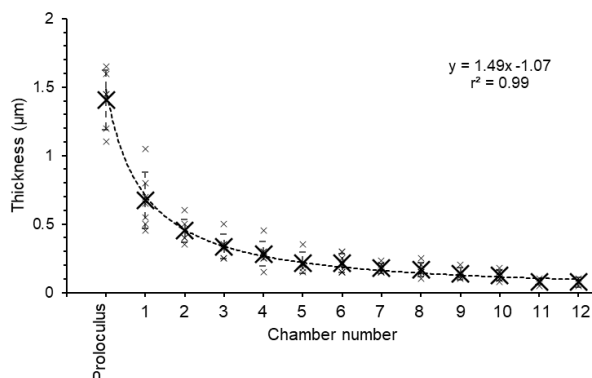


Figure 6: Plot representing the thickness of the Si layer as a function of the chamber number (numbered such as indicated on Fig. 4a) measured on 7 individuals. Measurements (minute black crosses) were averaged by chamber (big black crosses) and the standard deviation is represented by error bars. The black dotted line is a power law trend line based on averaged values.

230 3.2 Infrared spectra analyses

For all three *B. spissa* specimens and all chambers, FTIR spectra (Fig. 7) displayed a strong absorption band at $\sim 1070\text{ cm}^{-1}$ with an associated shoulder at $\sim 1250\text{ cm}^{-1}$ that are attributed to the asymmetric Si-O-Si stretching vibrations (Socrates, 2004; Larkin, 2011). The broad band at 3400 cm^{-1} and at $\sim 1635\text{ cm}^{-1}$ are ascribed to the O-H stretching of absorbed water, matching with opal. The IR spectra from the proloculus showed a broader band with a shoulder at $\sim 1250\text{ cm}^{-1}$, while a small peak from C-H stretching was observed at $\sim 2930\text{ cm}^{-1}$ in spectra of the 8th chamber.

235

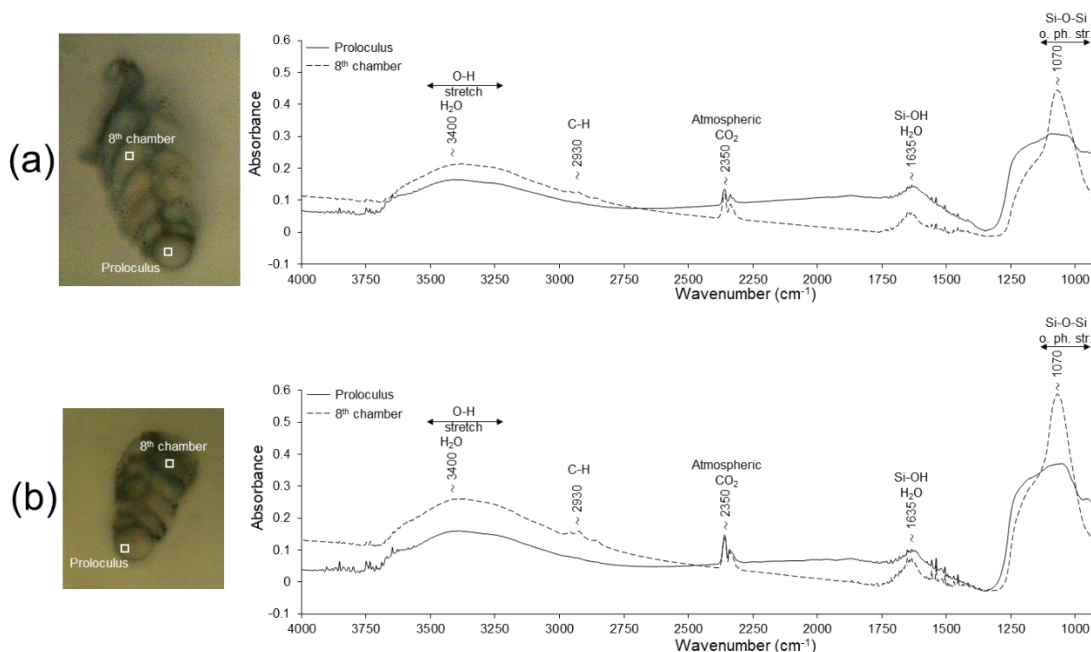
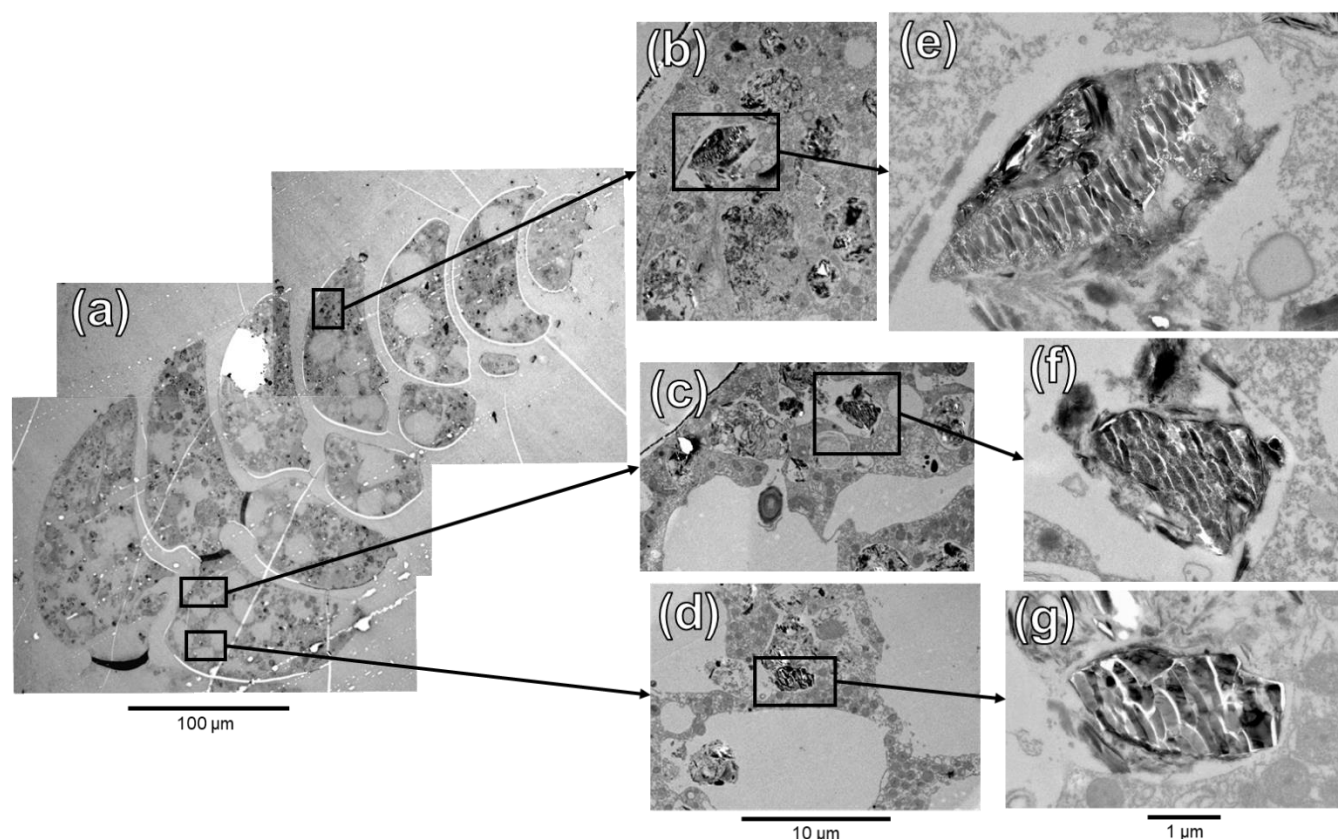


Figure 7: Examples of FTIR spectra measured on the proloculus (solid line) and the 8th chamber (dotted line) for two decalcified specimens (a and b) of *B. spissa*. o. ph. str. = out of phase stretching.



3.3 TEM imaging & STEM-EDS measurements



240

Figure 8: TEM images of ultra-thin section of *B. spissa* specimen (a). (b–d) Magnified regions of interest represented by black squares on (a). (e–g) Further magnified area of the black squares in (b), (c) and (d) respectively.

To investigate the putative organelles involved in silica deposition, TEM imaging of ultra-thin sections of *B. spissa* individuals were performed (Fig. 8). On a total of eight individuals imaged, structures filled with material presenting the characteristic conchoidal fracture pattern of silicon made material (Fig. 8b–g) were observed in two individuals. This conchoidal fracture pattern when sectioned with a diamond knife was also clear on the Si layer coating the inside part of the calcitic shell, which was visible on all eight specimens (Supplementary Fig. 2). Note that the aspect of these structures on TEM images is presumably denatured during sample preparation, such as previously reported for other silicifying organisms (Garrone et al., 1981).

245
250 STEM-EDS analyses indicated that the electron-dense material in these vesicles was mainly composed of silicon and showed a similar spectrum to the Si layer coating the internal part of the calcitic test (Supplementary Fig. 4). These organelles are remarkably resembling Silica Deposition Vesicles (SDVs) described in other biosilicifying organisms (Anderson, 1994; Foissner et al., 2009). The elemental composition of the content of these SDV-like organelles was different from vesicles filled with sediment material where Si was mostly associated with Al (aluminosilicates, such as feldspars which are abundantly



255 found in the sediment, Supplementary Fig. 4). The latter vesicles, filled with sediment and organic detritus, are abundantly occurring in the cytoplasm of *B. spissa* and represent food vacuoles (Goldstein & Corliss, 1994).

3.4 Isotopic analyses

260 The calcite mass of dissected samples ranged between 0.2 μg to 2.9 μg for proloculus side and 1.1 μg to 13.6 μg for apertural side (Supplementary Table 2). The proloculus side of dissected samples exhibited low $\delta^{18}\text{O}$ values between 0.13‰ to +3.09‰ compared with the aperture side which was ranging from +2.11‰ to +3.11‰. The $\delta^{18}\text{O}$ values of aperture side are comparable with isotopic equilibrium value of calcite at the depth of 1100 m in the Sagami Bay (Ishimura et al., 2012). Specimens exhibiting low $\delta^{18}\text{O}$ values also represent low $\delta^{13}\text{C}$ values. This trend was observed both for microspheric and macrospheric individuals (Supplementary Fig. 5). Lower $\delta^{18}\text{O}$ and $\delta^{13}\text{C}$ values were typically found in smaller (i.e., younger) specimens, having a test length ranging from 200 to 400 μm (Supplementary Fig. 6).

265 4 Discussion

4.1 Composite test made of calcite and opal

The Si layer, which was systematically observed in all studied *B. spissa*, is composed of biogenic opal (amorphous hydrated silica, $\text{SiO}_2 \cdot n\text{H}_2\text{O}$). This was firstly indicated by the cross-sections of the silicon-rich layer exposed by diamond knife cutting (cryo-SEM and TEM images), both showing a conchoidal fracture pattern (Fig. 5e & Supplementary Fig. 2), typical from 270 amorphous glass and well known from a variety of silicon-using organisms (see review in Garrone et al., 1981). This was further confirmed by FTIR spectra obtained on decalcified empty tests (translucid, dead), which were perfectly matching reference opal (Lowenstam, 1971), diatom frustules (Stefano et al., 2005) and diatomite (Reka et al., 2021) spectra. This is congruent with previous measurements on *Miliammellus legis* in Resig et al. (1980), for which the test material spectra also matched the opal reference of Lowenstam (1971).

275 The opal layer coating the inside part of the calcitic test of *B. spissa* seems composed of homogeneous material, without any visible sub-structures even on high resolution SEM images. This is different from *M. legis*, for which the test, made entirely of opal, is formed by a median layer (18 μm thick) composed of fused tubular rods randomly arranged in three-dimensional open mesh, framed by an inner and an outer layer (1 μm thick each), both composed of tightly packed rods sheets parallel to the inner and outer surface of the shell, respectively (Resig et al., 1980). These morphological and structural differences suggest 280 different precipitation processes between the two genera, such as it is the case for the carbonated test in Miliolida and Rotaliida, to which *Miliammellus* and *Bolivina* respectively belong (Parker, 2017; Dubicka, 2019).

In *B. spissa*, the opal layer thickness was constant within each chamber but was not equivalent between chambers in a given individual, always being the thickest in the proloculus and becoming thinner toward the newer chambers at the apertural side of the test. This decreasing trend in thickness is analogue to the calcitic test in Foraminifera having a lamellar wall (such as 285 *Bolivina*), which cover the entire test with new calcitic material (i.e., outer lamellae) when adding a new chamber, resulting in



a decreasing thickness of the calcitic test from the proloculus toward the newest chamber (Hansen, 2003). In some of our *B. spissa* specimens, we could observe such a decreased outer lamellae thickness toward external calcite layers on cryo-SEM images. The opal layer thickness from the proloculus towards the apertural side of the test follows an inverse power law (Fig. 6), suggesting that it is resulting from an ontogenetic effect. This decreasing thickness trend similarity in both calcite and opal, coupled to the observation of opal coating in young specimens (i.e., with few chambers), indicates that the opal layer is not formed during a single event but during multiple discrete steps, possibly likewise the precipitation pattern for the calcitic test. However, even in the proloculus where its thickness is maximum, no layered sub-structures were visible in the opal layer. After decalcification, the few last chambers on the apertural side were always collapsed or absent (Fig. 2), either because the opal layer was too thin to maintain its chamber-shaped structure or because of its absence in the newest part of the test. This is corroborated by cryo-SEM and TEM images observations, where no opal layer was visible in the newest chamber(s). The absence of opal layer in the newest calcified chambers indicates that its formation must occur afterward the precipitation of the calcitic shell.

4.2 Is it precipitated by the foraminifera itself?

Several observations indicate that the opal layer is secreted by the foraminifera itself and is not due to specific environmental conditions or any other passive process(es):

1. The layer is systematically present in all *B. spissa* sampled during two consecutive years (May and October 2022 and May 2023) and isolated from different depth intervals in the sediment, hence exposed to different environmental conditions (e.g., oxic/anoxic).
2. The layer only coats the inside part of the calcitic shell, suggesting that it is resulting from a mechanism taking place inside the calcitic test (i.e., in the cell and not in the surrounding water).
3. The layer is observed in living specimens, showing that the deposition process occurs when the individual is alive.
4. The layer is not observed in any other species found at the same site such as *Uvigerina*, *Chilostomella* or *Bulimina* genera, indicating that opal formation in *B. spissa* is not the result of a passive process.
5. The smooth and homogeneous aspect of the layer suggests that it is resulting from a precipitation process and not from an aggregation of particles from allochthonous origin (e.g., sediment or biogenic but previously secreted by another organism and subsequently incorporated by the foraminifer).
6. The opal layer thickness follows an allometric relationship (i.e., inverse power law), from the proloculus (thick) to newer chambers (thin), commonly found in organisms' growth pattern and suggesting that the layer is resulting from an ontogenetic process, analogous to the secreted calcitic test.

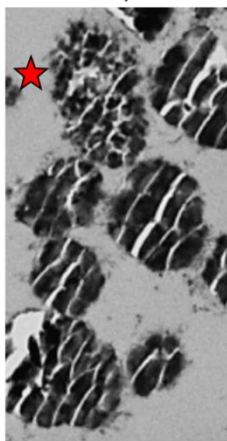
Supplementary TEM observations of peculiar organelles occurring in the cytoplasm and filled with similar material to opal layer (i.e., typical conchoidal fracture pattern on TEM images and EDS spectra indicating opal composition, Fig. 8 & Supplementary Fig. 4) further corroborate that the foraminifer secrete the opal layer itself. These organelles are strikingly resembling Silica Deposition Vesicles (SDVs), involved in the secretion of opal in diatom's frustule (Drum & Pankratz, 1964)



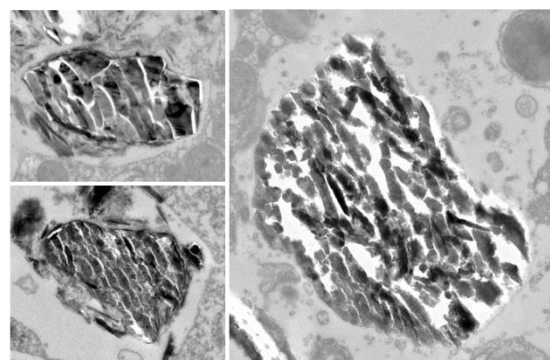
or the shell building of other organisms in the SAR group (Anderson, 1994; Foissner et al., 2009; Fig. 9) to which Foraminifera
320 belong. While *B. spissa* was shown to feed selectively on fresh phytodetritus transported from the surface ocean (e.g., diatoms,
Nomaki et al., 2006), the aspect of these organelles greatly differs from typical diatom frustules ingested by foraminifera (e.g.,
see Fig. 9D in Jauffrais et al., 2018, Fig. 4D in Goldstein & Corliss, 1994; Supplementary Fig. 7 in this study) or sponge spicule
(Garrone et al., 1981) indicating that they do not represent remains from these organisms. We consider that these organelles
are SDVs (Fig. 8 and 9), which were never reported before in Foraminifera (see review in LeKieffre et al., 2018). The
325 observation of these SDVs-like organelles in two over eight individuals analysed in total supports the hypothesis that the opal
deposition process takes place intermittently, or that these organelles occur rather rarely in the cytoplasm of *B. spissa*. SDVs-
like organelles were observed in new and older chambers at the same time (Fig. 8), suggesting that the opal layer deposition
might occur simultaneously in different chambers, resulting in thicker layers in older chambers. These organelles were
observed in individuals from 1-2 cm depth interval in the sediment, where oxygen is absent (Glud et al., 2009), suggesting that
330 opal precipitation may occur in anoxic settings. Further analyses, such as a transcriptomic study targeting genes involved
directly in silica precipitation or biosilicification, are necessary to conclude about the exact nature of these organelles.
The existence of a secreted opal layer coating the inside part of the calcitic test highlights a new biosilicification process in *B.*
spissa, making this species the first Rotaliida able to secrete opal and the first Foraminifera able to precipitate both materials
(i.e., calcite and opal) ever reported in our knowledge.

Ciliate SDVs
Maryna umbrellata
(Foissner et al., 2009)

Final developmental stage
Silicon granules showing typical
conchoidal fracture pattern of glass.
One of the granule was pulverized by
the diamond knife (red star)



Putative Foraminifera SDVs
Bolivina spissa
(this study)



335

Figure 9: TEM images showing the final development stage of the silicon granules in SDVs in the ciliate *Maryna umbrellata* (modified from Foissner et al., 2009) and organelles in *B. spissa* exhibiting similar aspect, hence representing putative SDVs. Note the scale difference, which is two times larger for *B. spissa* than for the ciliate.



The only other known biosilicifying Foraminifera is *M. legis* (Miliolida, Burmistrova, 1978), which is branching relatively far
340 from *Bolivina* (Rotaliida) in phylogenetic trees based on 18S rRNA (e.g., Pawlowski et al., 2013) or multi-gene phylogenies
(Groussin et al., 2011; Krabberød et al., 2017; Sierra et al., 2022, Supplementary Fig. 8a). These phylogenetic relationships,
nesting Rotaliida and Miliolida in naked foraminifers, suggests that biosilicification was acquired independently throughout
their evolution history. Similarly, it was already suggested that different test organisation/composition and calcification
pathways likely emerged multiple times during foraminiferal evolution in different foraminiferal orders, especially between
345 Rotaliida and Miliolida (Groussin et al., 2011; Pawlowski et al. 2013; Holzmann & Pawlowski, 2017; Sierra et al., 2022, de
Nooijer et al., 2023). The distinct aspect and microstructure of the opaline shell found in *B. spissa* compared to *M. legis*
supports the idea that this trait emerged independently in both *Bolivina* and *Miliammellus*. However, we cannot exclude the
hypothesis that biosilicification was inherited from a common ancestor (of rhizarians for instance) and that this trait was lost
in most of other Foraminifera represents. *SIT* genes putatively inherited from a common eukaryotic ancestor were already
350 identified in other well studied rotaliid Foraminifera that are not known to exhibit any opaline silica structures (i.e., *Ammonia*,
Elphidium and *Rosalina*, Marron et al., 2016, Supplementary Fig. 8b). This finding confirms that the presence of *SIT* genes
does not necessarily imply the capacity to precipitate opaline silica and rather corroborates the common ancestor hypothesis.
To investigate the exact origin of biosilicification in Foraminifera from an evolutionary point of view, further extensive
phylogenetic studies including *M. legis* are urged.

355 **4.3 Function(s) of the opal layer**

Foraminiferal test was proposed to serve various functions such as protection against predation, buoyancy control, or
facilitation of reproduction. Undoubtedly, the test also acts as protective physical barrier against unfavourable physical or
chemical conditions of the environment (Marszalek et al., 1969; Wetmore, 1987).

The only other foraminifer having an opaline test, *M. legis*, is found in relatively deep habitats (> 4400 m depth, Burmistrova,
360 1978; Resig et al., 1980) below the Carbonate Compensation Depth (CCD) where calcitic foraminifera are very rare (Resig et
al., 1980; Gooday et al., 2008). This suggests that secreting an opaline test could be an adaptation in environments in which
producing and maintaining a calcitic shell is challenging. However, *B. spissa* specimens in the present study were found at
much shallower depths (1410 m) well above the CCD (~ 4500-5000 m depth in the northwest Pacific, Chen et al., 1988), in
samples where other calcitic species occur abundantly and without any visible sign of dissolution. This indicates that
365 calcification is not limiting in these environments and suggests that the opaline and calcitic parts of the test serve different
and/or complementary function(s).

Diatom frustules, made of opal, are reportedly known to achieve incredible mechanical properties regarding their light weight
and strength leading to remarkable structural integrity (among other functions, Hamm et al., 2003; Knoll & Kotrc, 2015; Aitken
et al., 2016). Even if we did not observe any microstructures in the opal layer of *B. spissa* such as in Diatom's frustule, it is
370 plausible that the opal layer may serve as a supplementary mechanical support for the calcitic shell, enhancing the mechanical
integrity of the entire test. While this hypothesis is not supported by the occurrence of other species having a more fragile test

375 compared to *B. spissa* at the same location, such as *Chilostomella*, it still needs to be invalidated with measurements. Achieving a better mechanical resistance regarding compressive forces could represent an advantage in the context of protection against potential predation. This might be especially true for propagules or juveniles, since the opal layer is the thickest in old chambers at the proloculus side.

380 The thick opal layer in the proloculus might indicate a function associated with propagules dispersion. Compared to calcite, opal has a lower density (2.7 g.cm^{-3} and $1.9\text{-}2.2 \text{ g.cm}^{-3}$, respectively, Mukherjee, 2012), which could facilitate resuspension, movements, and/or propagation of juveniles by decreasing the density of young tests compared to a test of equivalent thickness made only of calcite. Some benthic foraminiferal species are hypothesised to have a floating propagule stage to insure long-
385 distance dispersal to different habitats (Alve & Goldstein, 2010). Alternatively, another *Bolivina* species, *Bolivina variabilis*, was reported as having a tychopelagic life strategy and being able to grow and calcify in benthic and in planktic settings depending on its ontogenetic stage (Darling et al., 2009; Kucera et al., 2017). The low $\delta^{18}\text{O}$ in the proloculus part of *B. spissa* (Supplementary Fig. 6 and 7) could indicate that juvenile specimens did calcify in a higher temperature environment compared to adult chambers, such as it is the case for the congeneric *B. variabilis* (Darling et al., 2009). However, the isotopic shift
385 between old and new chambers was not observed systematically in *B. spissa*, even among small individuals. Finally, the fact that an opal layer was not observed in decalcified *B. variabilis* (Supplementary Fig. 9) does not support the hypothesis that the opal layer observed in *B. spissa* could be involved in buoyancy function.

Opaline silica is acid-resistant and ~ 5 times harder to abrasion than calcite (Mukherjee, 2012). These two parameters might be of great value regarding protection against foraminiferivory (Hickman & Lipps, 1983). For instance, parasitic Foraminifera
390 were reported to be able to drill holes into the shell of bivalve by corrosion (i.e., dissolution, Cedhagen, 1994) and into the calcitic test of other Foraminifera species (by unknown mechanism, Hallock & Talge, 1994). Drilling by mechanical abrasion, presumably the result of predation by nematodes, was also found on foraminiferal tests belonging to *Rosalina* and *Bolivina* genera (Sliter, 1971). Additionally, selective predation on a Foraminifera from the Galapagos hydrothermal mounds by a naticid gastropod was reported by Arnold et al. (1985) and other unknown organisms were suggested to bore holes into
395 foraminiferal tests (Nielsen, 1999; Hickman & Lipps, 1983). Drilling strategies, either by chemical etching or mechanical abrasion, would be much more difficult or even inefficient against an opal layer, which would act as a protection layer preventing predators to access the cell content. Foraminifera in the Sagami Bay were shown to be potential prey for a variety of metazoans (e.g., molluscs, copepods, or nematodes, Nomaki et al., 2008), supporting the protection against predation hypothesis for *Bolivina* in this study. In case of complete ingestion by another organism (deliberate or fortuitous, e.g., Herbert,
400 1991; Hickman & Lipps, 1993; Lipps, 1983), it was suggested that some Foraminifera may survive relatively short passage in the gut by retracting in their test (Culver & Lipps, 2003), and the opaline silica layer may further help to avoid complete dissolution of the test in that specific case. Environmental SEM observations performed on another *Bolivina* morphospecies sampled from a nearby site in the Sagami Bay (Off Misaki, 740 m depth, $35^{\circ}04.30' \text{ N } 139^{\circ}32.50' \text{ E}$) indicate that it possesses comparable structures to *B. spissa* underlying the calcitic test after decalcification (Supplementary Fig. 10). While these
405 observations were only made on few dead specimens, we sometimes observed such predatory marks on their tests, with the



calcitic test being totally bored but with an underlying layer incompletely pierced (Supplementary Fig. 11). While these observations were made on a different *Bolivina* morphospecies, it suggests that protection from drilling strategy occur at a nearby location for the same genus. However, additional studies are necessary to confirm the exact nature of the structure exposed after decalcification in this different morphospecies and the origin of these borings.

410 We hypothesise that a plausible function of this opal layer coating the inside part of the calcitic shell would be an anti-predatory function, efficient against chemical or abrasive boring attacks, and potentially increasing the overall strength of the test in case of important compressive mechanical stress. Further investigations are needed to validate this hypothesis and define potential other(s), and perhaps non-exclusive, function(s).

4.4 Implication(s) for palaeoproxies and biogeochemical cycles

415 Compared to the aperture side of *B. spissa* where C and O isotopic compositions were almost close to equilibrium values, lower calcitic $\delta^{13}\text{C}$ and $\delta^{18}\text{O}$ values were principally observed at the proloculus side where the Si layer is the thickest. Moreover, the isotopic values of the proloculus side may be overwrite/diluted by the deposition of secondary calcite added during growth, lowering even further the $\delta^{18}\text{O}$ and $\delta^{13}\text{C}$ isotopic ratios that were measured in this study. This is confirmed by the fact that small specimens (i.e., with fewer chambers, younger) showed lower $\delta^{13}\text{C}$ and $\delta^{18}\text{O}$ values compared to larger specimens (i.e.,
420 with more chambers, older). These offsets can be explained by either “vital effects” during calcification or different habitat temperature during juvenile stage. The higher silicification observed on the proloculus side compared to the aperture side may have altered the cytoplasmic activity and/or resource partitioning regarding C and O in the cell, explaining the differences in isotopic composition between old and new chambers. Ishimura et al. (2012) suggested that the variations of intracellular chemistry affect the isotopic composition of the calcite shell. This may result from the more intense Si precipitation on the proloculus side (thicker opal layer) compared to the apertural side of the test in *B. spissa*. Additionally, the presence of an opaline layer might possibly influence proxy calibrations and their interpretations by mixing the measured calcite signal with the opal signal, such as suggested for sedimentary silicate grains incorporated within the calcite of *M. barleeanus* (Borrelli et al., 2018). The test composition of calcitic foraminifera is widely used for palaeoreconstruction and palaeoproxy purpose (e.g., Zachos et al., 2001; Katz et al., 2010) and *B. spissa* was already used in this context (Glock et al., 2012; Koho et al., 2017).
425 Therefore, refined geochemical composition analyses of the opaline layer, not done in our study, are necessary to assess its impact in the context of the use of *Bolivina* shells geochemical palaeoproxy. On the other hand, the presence of this opaline layer may open a whole new opportunity to develop novel proxies based on the glassy part of *B. spissa* test, especially in oxygen depleted environments. Such proxies exist for instance for diatoms, silicifying sponges or radiolarians, for which the isotopic composition may be used to trace dissolved silica concentration, pH or nitrate utilisation through geological times
430 (e.g., De La Rocha, 2006; Hendry et al., 2010; Donald et al., 2020; Trower et al., 2021).

Bolivina spissa is a cosmopolitan shallow infaunal species regularly reported at several different locations in the north-east Pacific such as the Santa Monica Basin, Monterey Bay cold-seeps or at the Cascadia convergent margin (e.g., Cushman, 1926; Bernhard et al., 2001; Heinz et al., 2005; Keating-Bitongo & Payne, 2017) as well as in the south-east Pacific at the Peruvian



margin (Glock et al., 2011). The species is also found in the north-west Pacific around Japan (Kitazato et al., 2000; Nomaki et al., 2006; Glud et al., 2009; Fontanier et al., 2014; Koho et al., 2017) and in the Okhotsk Sea (Bubenshchikova et al., 2008). Foraminifera are known to be major protagonists contributing to the organic and inorganic carbon cycle (OM degradation e.g., Gooday et al., 1992; Moodley et al., 2000; carbonate production, e.g., Langer, 2008) and nitrogen cycle (for denitrifying species such as *B. spissa*, e.g., Pina-Ochoa et al., 2010; Xu et al., 2017; Glock et al., 2019; Woehle et al., 2022). The wide geographic distribution and abundance of *B. spissa* emphasise its potential to be a good palaeoproxy using its opaline test and for global nitrogen cycle. If silicification in foraminifers was finally found to be more widespread than previously known, either among the genus *Bolivina* or possibly among other Foraminifera genera, this group could also have a substantial but overlooked role in silicon cycling, adding up to the already significant role of other Rhizaria in this cycle (Llopis Monferrer et al., 2020). Overall, silicifying Foraminifera may represent a critical component to better understand global Si cycling, which is in turn crucial to comprehend the functioning of other biogeochemical cycles, biological carbon pump or marine food webs (Tréguer et al., 2021).

5 Conclusions

We report that the Foraminifera *Bolivina spissa* exhibits a composite test made of an opal layer coating internal part of the calcitic test. The thickness pattern of the opal layer, thick in the proloculus and thinning toward newer chambers, coupled to the identification of organelles involved in silica precipitation found for the first time in Foraminifera, ascribed to Silica Deposition Vesicles (SDVs), indicate that the *B. spissa* can silicify by itself. The deposition of opal appears to be discontinuous and to take place afterward calcite precipitation phases, while occurring in different chambers at the same time. We presume that the opal layer may serve as a protection barrier against predators able to drill holes chemically or mechanically in the calcitic test of Foraminifera. However, others (non-exclusive) functions could exist and are still to be investigated further. The presence of this unnoticed opal layer below the calcitic test in the cosmopolitan *B. spissa* raise the question of silicification extend in Foraminifera. The only other known silicifying species, branching relatively far on phylogenetic trees, belongs to another foraminiferal class, and preliminary observations on another *Bolivina* morphospecies exhibiting analogous structures below calcite could indicate that this trait may be more widespread than previously assumed. While the presence of this opal layer may influence palaeoceanographic reconstruction using test composition, it may lead to the development of new palaeoproxy(ies) based on this layer. Finally, if silicification was found to be more widespread than previously known, it would probably make Foraminifera significant, so far overlooked, actors regarding the Si cycle at global scale.

Data availability

Raw data are available in the supplementary material attached to this manuscript.



Author contribution

Julien Richirt: conceptualisation, sampling, environmental SEM samples preparation and data acquisition, data interpretation, original draft writing. **Satoshi Okada:** sampling, cryo-SEM and FTIR samples preparation and data acquisition, data interpretation. **Yoshiyuki Ishitani:** sampling, data interpretation. **Katsuyuki Uematsu:** TEM samples preparation and data acquisition. **Akihiro Tame:** TEM samples preparation. **Kaya Oda:** Foraminifera picking, samples preparations. **Noriyuki Isobe:** FTIR data acquisition, data interpretation. **Toyoho Ishimura:** isotopic data acquisition and interpretation. **Masashi Tsuchiya:** data interpretation. **Hidetaka Nomaki:** conceptualisation, sampling, data interpretation. All co-authors participated in the writing, review, and editing process.

Competing interest

The authors declare that they have no competing interest.

Acknowledgments

We are grateful to the captains, crew members and onboard scientists of the research vessel R/V *Yokosuka* as well as the operation team of HOV *Shinkai 6500* for their help during samples collection. We would like to thank Takazo Shibuya (JAMSTEC) for his help regarding FTIR measurements. This work was supported by the Japan Society for the Promotion of Science (JSPS) funding P21729 and 21H01202.

References

- Aitken, Z. H., Luo, S., Reynolds, S. N., Thaulow, C., and Greer, J. R.: Microstructure provides insights into evolutionary design and resilience of *Coscinodiscus* sp. frustule, *Proceedings of the National Academy of Sciences*, 113, 2017–2022, <https://doi.org/10.1073/pnas.1519790113>, 2016.
- Alve, E. and Goldstein, S. T.: Dispersal, survival and delayed growth of benthic foraminiferal propagules, *Journal of Sea Research*, 63, 36–51, <https://doi.org/10.1016/j.seares.2009.09.003>, 2010.
- Anderson, O. R.: Cytoplasmic origin and surface deposition of siliceous structures in Sarcodina, *Protoplasma*, 181, 61–77, <https://doi.org/10.1007/BF01666389>, 1994.
- Arnold, A. J., d’Escrivan, F., and Parker, W. C.: Predation and avoidance responses in the foraminifera of the Galapagos hydrothermal mounds, *Journal of Foraminiferal Research*, 15, 38–42, <https://doi.org/10.2113/gsjfr.15.1.38>, 1985.
- Bernhard, J. M., Buck, K. R., and Barry, J. P.: Monterey Bay cold-seep biota: Assemblages, abundance, and ultrastructure of living foraminifera, *Deep Sea Research Part I: Oceanographic Research Papers*, 48, 2233–2249, [https://doi.org/10.1016/S0967-0637\(01\)00017-6](https://doi.org/10.1016/S0967-0637(01)00017-6), 2001.



- Borrelli, C., Panieri, G., Dahl, T. M., and Neufeld, K.: Novel biomineralization strategy in calcareous foraminifera, *Sci Rep*, 8, 10201, <https://doi.org/10.1038/s41598-018-28400-2>, 2018.
- Brady, Expedition (1872-1876), C., Britain, G., Buchan, A., Huxley, T. H., Murray, J., Nares, G. S., Nares, G. S., Pelseneer, P., Thomson, C. W., Thomson, F. T., Thomson, F. T., and Challenger (Ship): Report on the scientific results of the voyage of H.M.S. Challenger during the years 1873-76 under the command of Captain George S. Nares and Captain Frank Tourle Thomson, R.N, Neill, Edinburgh, 858 pp., 1884.
- Brümmer (auth.), F. and Müller (eds.), P. D. W. E. G.: *Silicon Biomineralization: Biology — Biochemistry — Molecular Biology — Biotechnology*, 1st ed., Springer-Verlag Berlin Heidelberg, 2003.
- Bubenshchikova, N., Nürnberg, D., Lembke-Jene, L., and Pavlova, G.: Living benthic foraminifera of the Okhotsk Sea: Faunal composition, standing stocks and microhabitats, *Marine Micropaleontology*, 69, 314–333, <https://doi.org/10.1016/j.marmicro.2008.09.002>, 2008.
- Burki, F., Roger, A. J., Brown, M. W., and Simpson, A. G. B.: The New Tree of Eukaryotes, *Trends in Ecology & Evolution*, 35, 43–55, <https://doi.org/10.1016/j.tree.2019.08.008>, 2020.
- Burmistrova, I. I.: K stratigrafii glubokovodnykh osadkov vostochnoy chasti Indiyaskogo Okeana po bentosnym foraminiferam [On the stratigraphy of deep sea deposits in the eastern part of the Indian Ocean, based on benthic foraminifera], in *Morskaya Mikropaleontologiya*, Moscow: Akademiya Nauk SSSR, Okeanograficheskaya Komissiya, 163–170, 1978.
- Cedhagen, T.: Taxonomy and biology of *Hyrrokin sarcophaga* gen. et sp. n., a parasitic foraminiferan (Rosalinidae), *Sarsia*, 79, 65–82, <https://doi.org/10.1080/00364827.1994.10413549>, 1994.
- Cesbron, F., Geslin, E., Jorissen, F. J., Delgard, M. L., Charrieau, L., Deflandre, B., Jézéquel, D., Anschutz, P., and Metzger, E.: Vertical distribution and respiration rates of benthic foraminifera: Contribution to aerobic remineralization in intertidal mudflats covered by *Zostera noltei* meadows, *Estuarine, Coastal and Shelf Science*, 179, 23–38, <https://doi.org/10.1016/j.ecss.2015.12.005>, 2016.
- Chen, C. T. A., Feely, R. A., and Gendron, J. F.: *Lysocline, Calcium Carbonate Compensation Depth, and Calcareous Sediments in the North Pacific Ocean*, 1988.
- Culver, S. J.: Early Cambrian Foraminifera from West Africa, *Science*, 254, 689–691, <https://doi.org/10.1126/science.254.5032.689>, 1991.
- Culver, S. J. and Lipps, J. H.: Predation on and by Foraminifera, in: *Predator—Prey Interactions in the Fossil Record*, edited by: Kelley, P. H., Kowalewski, M., and Hansen, T. A., Springer US, Boston, MA, 7–32, https://doi.org/10.1007/978-1-4615-0161-9_2, 2003.
- Cushman, J. A.: Some Pliocene *Bolivinas* from California, *Contributions from the Cushman laboratory for foraminiferal research*, 2, 40–47, 1926.
- Darling, K. F., Thomas, E., Kasemann, S. A., Sears, H. A., Smart, C. W., and Wade, C. M.: Surviving mass extinction by bridging the benthic/planktic divide, *Proceedings of the National Academy of Sciences*, 106, 12629–12633, <https://doi.org/10.1073/pnas.0902827106>, 2009.



- 530 De La Rocha, C. L.: Opal-based isotopic proxies of paleoenvironmental conditions, *Global Biogeochemical Cycles*, 20, <https://doi.org/10.1029/2005GB002664>, 2006.
- Donald, H. K., Foster, G. L., Fröhberg, N., Swann, G. E. A., Poulton, A. J., Moore, C. M., and Humphreys, M. P.: The pH dependency of the boron isotopic composition of diatom opal (*Thalassiosira weissflogii*), *Biogeosciences*, 17, 2825–2837, <https://doi.org/10.5194/bg-17-2825-2020>, 2020.
- 535 Drum, R. W. and Pankratz, H. S.: Post mitotic fine structure of *Gomphonema parvulum*, *J Ultrastruct Res*, 10, 217–223, [https://doi.org/10.1016/s0022-5320\(64\)80006-x](https://doi.org/10.1016/s0022-5320(64)80006-x), 1964.
- Dubicka, Z.: Chamber arrangement versus wall structure in the high-rank phylogenetic classification of Foraminifera, *Acta Palaeontologica Polonica*, 64, <https://doi.org/10.4202/app.00564.2018>, 2019.
- Echols, R. J.: Distribution of Foraminifera in Sediments of the Scotia Sea Area, Antarctic Waters, in: *Antarctic Oceanology I*, American Geophysical Union (AGU), 93–168, <https://doi.org/10.1029/AR015p0093>, 1971.
- 540 Ehrlich, H. L., Newman, D. K., and Kappler, A. (Eds.): Ehrlich’s Geomicrobiology, 6th edition., CRC Press, 656 pp., 2016.
- Foissner, W., Weissenbacher, B., Krautgartner, W.-D., and Lütz-Meindl, U.: A Cover of Glass: First Report of Biomineralized Silicon in a Ciliate, *Maryna umbrellata* (Ciliophora: Colpodea), *J Eukaryot Microbiol*, 56, 519–530, <https://doi.org/10.1111/j.1550-7408.2009.00431.x>, 2009.
- 545 Fontanier, C., Duros, P., Toyofuku, T., Oguri, K., Koho, K. A., Buscail, R., Gremare, A., Radakovitch, O., Deflandre, B., De Nooijer, L. J., Bichon, S., Goubet, S., Ivanovsky, A., Chabaud, G., Menniti, C., Reichart, G.-J., and Kitazato, H.: living (stained) deep-sea foraminifera off Hachinohe (NE Japan, western Pacific): environmental interplay in oxygen-depleted ecosystems, *The Journal of Foraminiferal Research*, 44, 281–299, <https://doi.org/10.2113/gsjfr.44.3.281>, 2014.
- Garrone, R., Simpson, T. L., and Pottu-Boumendil, J.: Ultrastructure and Deposition of Silica in Sponges, in: *Silicon and Siliceous Structures in Biological Systems*, edited by: Simpson, T. L. and Volcani, B. E., Springer, New York, NY, 495–525, https://doi.org/10.1007/978-1-4612-5944-2_17, 1981.
- 550 Glock, N., Eisenhauer, A., Milker, Y., Liebetrau, V., Schönfeld, J., Mallon, J., Sommer, S., and Hensen, C.: Environmental Influences on the Pore Density of *Bolivina Spissa* (Cushman), *Journal of Foraminiferal Research*, 41, 22–32, <https://doi.org/10.2113/gsjfr.41.1.22>, 2011.
- 555 Glock, N., Eisenhauer, A., Liebetrau, V., Wiedenbeck, M., Hensen, C., and Nehrke, G.: EMP and SIMS studies on Mn/Ca and Fe/Ca systematics in benthic foraminifera from the Peruvian OMZ: a contribution to the identification of potential redox proxies and the impact of cleaning protocols, *Biogeosciences*, 9, 341–359, <https://doi.org/10.5194/bg-9-341-2012>, 2012.
- Glock, N., Roy, A.-S., Romero, D., Wein, T., Weissenbach, J., Revsbech, N. P., Høglund, S., Clemens, D., Sommer, S., and Dagan, T.: Metabolic preference of nitrate over oxygen as an electron acceptor in foraminifera from the Peruvian oxygen
- 560 minimum zone, *PNAS*, 116, 2860–2865, <https://doi.org/10.1073/pnas.1813887116>, 2019.
- Glud, R. N., Thamdrup, B., Stahl, H., Wenzhoefer, F., Glud, A., Nomaki, H., Oguri, K., Revsbech, N. P., and Kitazato, H.: Nitrogen cycling in a deep ocean margin sediment (Sagami Bay, Japan), *Limnology and Oceanography*, 54, 723–734, <https://doi.org/10.4319/lo.2009.54.3.0723>, 2009.



- Goldstein, S. T. and Corliss, B. H.: Deposit feeding in selected deep-sea and shallow-water benthic foraminifera, *Deep Sea Research Part I: Oceanographic Research Papers*, 41, 229–241, [https://doi.org/10.1016/0967-0637\(94\)90001-9](https://doi.org/10.1016/0967-0637(94)90001-9), 1994.
- Gooday, A. J., Levin, L. A., Linke, P., and Heeger, T.: The Role of Benthic Foraminifera in Deep-Sea Food Webs and Carbon Cycling, in: *Deep-Sea Food Chains and the Global Carbon Cycle*, edited by: Rowe, G. T. and Pariente, V., Springer Netherlands, Dordrecht, 63–91, https://doi.org/10.1007/978-94-011-2452-2_5, 1992.
- Gooday, A. J., Nomaki, H., and Kitazato, H.: Modern deep-sea benthic foraminifera: a brief review of their morphology-based biodiversity and trophic diversity, *Geological Society, London, Special Publications*, 303, 97–119, <https://doi.org/10.1144/SP303.8>, 2008.
- Greenwood, N. N. and Earnshaw, A.: *Chemistry of the Elements*, Elsevier, 1365 pp., 1997.
- Groussin, M., Pawlowski, J., and Yang, Z.: Bayesian relaxed clock estimation of divergence times in foraminifera, *Molecular Phylogenetics and Evolution*, 61, 157–166, <https://doi.org/10.1016/j.ympev.2011.06.008>, 2011.
- Gupta, B. K. S.: *Modern Foraminifera*, Springer Science & Business Media, 368 pp., 2003.
- Hallock, P. and Talge, H.: A Predatory Foraminifer, *Floresina amphiphaga*, n. sp., from the Florida Keys, *Journal of Foraminiferal Research*, 24, 210–213, <https://doi.org/10.2113/gsjfr.24.4.210>, 1994.
- Hamm, C. E., Merkel, R., Springer, O., Jurkojc, P., Maier, C., Prectel, K., and Smetacek, V.: Architecture and material properties of diatom shells provide effective mechanical protection, *Nature*, 421, 841–843, <https://doi.org/10.1038/nature01416>, 2003.
- Hansen, H. J.: Shell construction in modern calcareous Foraminifera, in: *Modern Foraminifera*, edited by: Sen Gupta, B. K., Springer Netherlands, Dordrecht, 57–70, https://doi.org/10.1007/0-306-48104-9_4, 2003.
- Heinz, P., Sommer, S., Pfannkuche, O., and Hemleben, C.: Living benthic foraminifera in sediments influenced by gas hydrates at the Cascadia convergent margin, NE Pacific, *Marine Ecology Progress Series*, 304, 77–89, <https://doi.org/10.3354/meps304077>, 2005.
- Hendry, K. R., Georg, R. B., Rickaby, R. E. M., Robinson, L. F., and Halliday, A. N.: Deep ocean nutrients during the Last Glacial Maximum deduced from sponge silicon isotopic compositions, *Earth and Planetary Science Letters*, 292, 290–300, <https://doi.org/10.1016/j.epsl.2010.02.005>, 2010.
- Hendry, K. R., Marron, A. O., Vincent, F., Conley, D. J., Gehlen, M., Ibarbalz, F. M., Quéguiner, B., and Bowler, C.: Competition between Silicifiers and Non-silicifiers in the Past and Present Ocean and Its Evolutionary Impacts, *Frontiers in Marine Science*, 5, 2018.
- Herbert, D. G.: Foraminiferivory in a *Puncturella* (Gastropoda: Fissurellidae), *Journal of Molluscan Studies*, 57, 127–129, <https://doi.org/10.1093/mollus/57.1.127>, 1991.
- Hickman, C. S. and Lipps, J. H.: Foraminiferivory; selective ingestion of foraminifera and test alterations produced by the neogastropod *Olivella*, *Journal of Foraminiferal Research*, 13, 108–114, <https://doi.org/10.2113/gsjfr.13.2.108>, 1983.
- Holzmann, M. and Pawlowski, J.: An updated classification of rotaliid foraminifera based on ribosomal DNA phylogeny, *Marine Micropaleontology*, 132, 18–34, <https://doi.org/10.1016/j.marmicro.2017.04.002>, 2017.



- Ishimura, T., Tsunogai, U., and Gamo, T.: Stable carbon and oxygen isotopic determination of sub-microgram quantities of CaCO₃ to analyze individual foraminiferal shells, *Rapid Commun Mass Spectrom*, 18, 2883–2888, 600 <https://doi.org/10.1002/rcm.1701>, 2004.
- Ishimura, T., Tsunogai, U., and Nakagawa, F.: Grain-scale heterogeneities in the stable carbon and oxygen isotopic compositions of the international standard calcite materials (NBS 19, NBS 18, IAEA-CO-1, and IAEA-CO-8), *Rapid Commun Mass Spectrom*, 22, 1925–1932, <https://doi.org/10.1002/rcm.3571>, 2008.
- Ishimura, T., Tsunogai, U., Hasegawa, S., Nakagawa, F., Oi, T., Kitazato, H., Suga, H., and Toyofuku, T.: Variation in stable 605 carbon and oxygen isotopes of individual benthic foraminifera: tracers for quantifying the magnitude of isotopic disequilibrium, *Biogeosciences*, 9, 4353–4367, <https://doi.org/10.5194/bg-9-4353-2012>, 2012.
- Jauffrais, T., LeKieffre, C., Koho, K. A., Tsuchiya, M., Schweizer, M., Bernhard, J. M., Meibom, A., and Geslin, E.: Ultrastructure and distribution of kleptoplasts in benthic foraminifera from shallow-water (photic) habitats, *Marine Micropaleontology*, 138, 46–62, <https://doi.org/10.1016/j.marmicro.2017.10.003>, 2018.
- 610 Jones, R. W.: *Foraminifera and their Applications*, Cambridge University Press, 407 pp., 2013.
- Katz, M. E., Cramer, B. S., Franzese, A., Hönisch, B., Miller, K. G., Rosenthal, Y., and Wright, J. D.: Traditional and emerging geochemical proxies in foraminifera, *Journal of Foraminiferal Research*, 40, 165–192, <https://doi.org/10.2113/gsjfr.40.2.165>, 2010.
- Keating-Bitonti, C. R. and Payne, J. L.: Ecophenotypic responses of benthic foraminifera to oxygen availability along an 615 oxygen gradient in the California Borderland, *Marine Ecology*, 38, e12430, <https://doi.org/10.1111/maec.12430>, 2017.
- Kitazato, H., Shirayama, Y., Nakatsuka, T., Fujiwara, S., Shimanaga, M., Kato, Y., Okada, Y., Kanda, J., Yamaoka, A., Masuzawa, T., and Suzuki, K.: Seasonal phytodetritus deposition and responses of bathyal benthic foraminiferal populations in Sagami Bay, Japan: preliminary results from “Project Sagami 1996–1999,” *Marine Micropaleontology*, 40, 135–149, [https://doi.org/10.1016/S0377-8398\(00\)00036-0](https://doi.org/10.1016/S0377-8398(00)00036-0), 2000.
- 620 Knoll, A. H. and Kotrc, B.: *Protistan Skeletons: A Geologic History of Evolution and Constraint*, in: *Evolution of Lightweight Structures: Analyses and Technical Applications*, edited by: Hamm, C., Springer Netherlands, Dordrecht, 1–16, https://doi.org/10.1007/978-94-017-9398-8_1, 2015.
- Koho, K. A., de Nooijer, L. J., Fontanier, C., Toyofuku, T., Oguri, K., Kitazato, H., and Reichart, G.-J.: Benthic foraminiferal Mn / Ca ratios reflect microhabitat preferences, *Biogeosciences*, 14, 3067–3082, <https://doi.org/10.5194/bg-14-3067-2017>, 625 2017.
- Krabberød, A. K., Orr, R. J. S., Bråte, J., Kristensen, T., Bjørklund, K. R., and Shalchian-Tabrizi, K.: Single Cell Transcriptomics, Mega-Phylogeny, and the Genetic Basis of Morphological Innovations in Rhizaria, *Molecular Biology and Evolution*, 34, 1557–1573, <https://doi.org/10.1093/molbev/msx075>, 2017.
- Kucera, M., Silye, L., Weiner, A. K. M., Darling, K., Lübben, B., Holzmann, M., Pawlowski, J., Schönfeld, J., and Morard, 630 R.: Caught in the act: anatomy of an ongoing benthic–planktonic transition in a marine protist, *Journal of Plankton Research*, 39, 436–449, <https://doi.org/10.1093/plankt/fbx018>, 2017.



- Langer, M. R.: Assessing the Contribution of Foraminiferan Protists to Global Ocean Carbonate Production1, *Journal of Eukaryotic Microbiology*, 55, 163–169, <https://doi.org/10.1111/j.1550-7408.2008.00321.x>, 2008.
- Larkin, P.: *Infrared and Raman Spectroscopy: Principles and Spectral Interpretation*, Elsevier, 239 pp., 2011.
- 635 LeKieffre, C., Bernhard, J. M., Mabilieu, G., Filipsson, H. L., Meibom, A., and Geslin, E.: An overview of cellular ultrastructure in benthic foraminifera: New observations of rotalid species in the context of existing literature, *Marine Micropaleontology*, 138, 12–32, <https://doi.org/10.1016/j.marmicro.2017.10.005>, 2018.
- Llopis Monferrer, N., Boltovskoy, D., Tréguer, P., Sandin, M. M., Not, F., and Leynaert, A.: Estimating Biogenic Silica Production of Rhizaria in the Global Ocean, *Global Biogeochemical Cycles*, 34, e2019GB006286,
640 <https://doi.org/10.1029/2019GB006286>, 2020.
- Lowenstam, H. A.: Opal Precipitation by Marine Gastropods (Mollusca), *Science*, 171, 487–490, <https://doi.org/10.1126/science.171.3970.487>, 1971.
- Marron, A. O., Ratcliffe, S., Wheeler, G. L., Goldstein, R. E., King, N., Not, F., de Vargas, C., and Richter, D. J.: The Evolution of Silicon Transport in Eukaryotes, *Molecular Biology and Evolution*, 33, 3226–3248,
645 <https://doi.org/10.1093/molbev/msw209>, 2016.
- Marszalek, D. S., Wright, R. C., and Hay, W. W.: Function of the Test in Foraminifera, *Gulf Coast. Assoc. Geological Societies Trans.*, 19, 341–352, 1969.
- Mayerhöfer, T. G., Pahlow, S., Hübner, U., and Popp, J.: CaF₂: An Ideal Substrate Material for Infrared Spectroscopy?, *Anal. Chem.*, 92, 9024–9031, <https://doi.org/10.1021/acs.analchem.0c01158>, 2020.
- 650 Moodley, L., Boschker, H. T. S., Middelburg, J. J., Pel, R., Herman, P. M. J., Deckere, E. de, and Heip, C. H. R.: Ecological significance of benthic foraminifera: ¹³C labelling experiments, *Marine Ecology Progress Series*, 202, 289–295, <https://doi.org/10.3354/meps202289>, 2000.
- Mukherjee, S.: *Applied Mineralogy: Applications in Industry and Environment*, Springer Science & Business Media, 585 pp., 2012.
- 655 Murray, J. W.: *Ecology and Applications of Benthic Foraminifera*, Cambridge University Press, Cambridge, <https://doi.org/10.1017/CBO9780511535529>, 2006.
- Murray, J. W.: Biodiversity of living benthic foraminifera: How many species are there?, *Marine Micropaleontology*, 64, 163–176, <https://doi.org/10.1016/j.marmicro.2007.04.002>, 2007.
- Nagai, Y., Uematsu, K., Chen, C., Wani, R., Tyszka, J., and Toyofuku, T.: Weaving of biomineralization framework in rotalid
660 foraminifera: implications for paleoceanographic proxies, *Biogeosciences*, 15, 6773–6789, <https://doi.org/10.5194/bg-15-6773-2018>, 2018.
- Nielsen, K. S. S.: Foraminiferivory revisited: a preliminary investigation of holes in foraminifera, *Bulletin of the Geological Society of Denmark*, 45, 139–142, 1999.



- 665 Nomaki, H., Heinz, P., Nakatsuka, T., Shimanaga, M., Ohkouchi, N., Ogawa, N. O., Kogure, K., Ikemoto, E., and Kitazato, H.: Different ingestion patterns of ¹³C-labeled bacteria and algae by deep-sea benthic foraminifera, *Marine Ecology Progress Series*, 310, 95–108, <https://doi.org/10.3354/meps310095>, 2006.
- Nomaki, H., Ogawa, N. O., Ohkouchi, N., Suga, H., Toyofuku, T., Shimanaga, M., Nakatsuka, T., and Kitazato, H.: Benthic foraminifera as trophic links between phytodetritus and benthic metazoans: carbon and nitrogen isotopic evidence, *Marine Ecology Progress Series*, 357, 153–164, <https://doi.org/10.3354/meps07309>, 2008.
- 670 de Nooijer, L. J., Spero, H. J., Erez, J., Bijma, J., and Reichart, G. J.: Biomineralization in perforate foraminifera, *Earth-Science Reviews*, 135, 48–58, <https://doi.org/10.1016/j.earscirev.2014.03.013>, 2014.
- de Nooijer, L. J., Pacho Sampedro, L., Jorissen, F. J., Pawlowski, J., Rosenthal, Y., Dissard, D., and Reichart, G. J.: 500 million years of foraminiferal calcification, *Earth-Science Reviews*, 243, 104484, <https://doi.org/10.1016/j.earscirev.2023.104484>, 2023.
- 675 Parker, J. H.: Ultrastructure of the Test Wall in Modern Porcelaneous Foraminifera: Implications For the Classification of the Miliolida, *Journal of Foraminiferal Research*, 47, 136–174, <https://doi.org/10.2113/gsjfr.47.2.136>, 2017.
- Pawlowski, J., Holzmann, M., and Tyszka, J.: New supraordinal classification of Foraminifera: Molecules meet morphology, *Marine Micropaleontology*, 100, 1–10, <https://doi.org/10.1016/j.marmicro.2013.04.002>, 2013.
- Piña-Ochoa, E., Høglund, S., Geslin, E., Cedhagen, T., Revsbech, N. P., Nielsen, L. P., Schweizer, M., Jorissen, F., Rysgaard, S., and Risgaard-Petersen, N.: Widespread occurrence of nitrate storage and denitrification among Foraminifera and Gromiida, *PNAS*, 107, 1148–1153, <https://doi.org/10.1073/pnas.0908440107>, 2010.
- Reka, A. A., Pavlovski, B., Fazlija, E., Berisha, A., Pacarizi, M., Daghmehchi, M., Sacalis, C., Jovanovski, G., Makreski, P., and Oral, A.: Diatomaceous Earth: Characterization, thermal modification, and application, *Open Chemistry*, 19, 451–461, <https://doi.org/10.1515/chem-2020-0049>, 2021.
- 685 Resig, J. M., Lowenstam, H. A., Echols, R. J., and Weiner, S.: An extant opaline foraminifer: test ultrastructure, mineralogy, and taxonomy, in: *Studies in Marine Micropaleontology and Paleoecology: A Memorial Volume to Orville L. Bandy*, vol. 19, edited by: Sliter, W. V., Cushman Foundation for Foraminiferal Research, 0, 1980.
- Schindelin, J., Arganda-Carreras, I., Frise, E., Kaynig, V., Longair, M., Pietzsch, T., Preibisch, S., Rueden, C., Saalfeld, S., Schmid, B., Tinevez, J.-Y., White, D. J., Hartenstein, V., Eliceiri, K., Tomancak, P., and Cardona, A.: Fiji: an open-source platform for biological-image analysis, *Nat Methods*, 9, 676–682, <https://doi.org/10.1038/nmeth.2019>, 2012.
- 690 Sierra, R., Mauffrey, F., Cruz, J., Holzmann, M., Gooday, A. J., Maurer-Alcalá, X., Thakur, R., Greco, M., Weiner, A. K. M., Katz, L. A., and Pawlowski, J.: Taxon-rich transcriptomics supports higher-level phylogeny and major evolutionary trends in Foraminifera, *Molecular Phylogenetics and Evolution*, 174, 107546, <https://doi.org/10.1016/j.ympev.2022.107546>, 2022.
- Sliter, W. V.: Predation on benthic foraminifers, *Journal of Foraminiferal Research*, 1, 20–28, <https://doi.org/10.2113/gsjfr.1.1.20>, 1971.
- Socrates, G.: *Infrared and Raman Characteristic Group Frequencies: Tables and Charts*, John Wiley & Sons, 386 pp., 2004.



- Stefano, L. D., Stefano, M. D., Rea, I., Moretti, L., Bismuto, A., Maddalena, P., and Rendina, I.: Optical characterisation of biological nano-porous silica structures, in: *Nanophotonic Materials and Systems II, Nanophotonic Materials and Systems II*, 106–110, <https://doi.org/10.1117/12.619450>, 2005.
- 700 Toyofuku, T., Matsuo, M. Y., Nooijer, L. J. de, Nagai, Y., Kawada, S., Fujita, K., Reichart, G.-J., Nomaki, H., Tsuchiya, M., Sakaguchi, H., and Kitazato, H.: Proton pumping accompanies calcification in foraminifera, *Nat Commun*, 8, 1–6, <https://doi.org/10.1038/ncomms14145>, 2017.
- Tréguer, P. J., Sutton, J. N., Brzezinski, M., Charette, M. A., Devries, T., Dutkiewicz, S., Ehlert, C., Hawkings, J., Leynaert, A., Liu, S. M., Llopis Monferrer, N., López-Acosta, M., Maldonado, M., Rahman, S., Ran, L., and Rouxel, O.: Reviews and
705 syntheses: The biogeochemical cycle of silicon in the modern ocean, *Biogeosciences*, 18, 1269–1289, <https://doi.org/10.5194/bg-18-1269-2021>, 2021.
- Trower, E. J., Strauss, J. V., Sperling, E. A., and Fischer, W. W.: Isotopic analyses of Ordovician–Silurian siliceous skeletons indicate silica-depleted Paleozoic oceans, *Geobiology*, 19, 460–472, <https://doi.org/10.1111/gbi.12449>, 2021.
- Ujjié, Y., Ishitani, Y., Nagai, Y., Takaki, Y., Toyofuku, T., and Ishii, S.: Unique evolution of foraminiferal calcification to
710 survive global changes, *Science Advances*, 9, eadd3584, <https://doi.org/10.1126/sciadv.add3584>, 2023.
- Wetmore, K. L.: Correlations between test strength, morphology and habitat in some benthic foraminifera from the coast of Washington, *Journal of Foraminiferal Research*, 17, 1–13, <https://doi.org/10.2113/gsjfr.17.1.1>, 1987.
- Woehle, C., Roy, A.-S., Glock, N., Michels, J., Wein, T., Weissenbach, J., Romero, D., Hiebenthal, C., Gorb, S. N., Schönfeld, J., and Dagan, T.: Denitrification in foraminifera has an ancient origin and is complemented by associated bacteria, *Proceedings of the National Academy of Sciences*, 119, e2200198119, <https://doi.org/10.1073/pnas.2200198119>, 2022.
- 715 Xu, Z., Liu, S., Xiang, R., and Song, G.: Live benthic foraminifera in the Yellow Sea and the East China Sea: vertical distribution, nitrate storage, and potential denitrification, *Marine Ecology Progress Series*, 571, 65–81, <https://doi.org/10.3354/meps12135>, 2017.
- Zachos, J., Pagani, M., Sloan, L., Thomas, E., and Billups, K.: Trends, Rhythms, and Aberrations in Global Climate 65 Ma to
720 Present, *Science*, 292, 686–693, <https://doi.org/10.1126/science.1059412>, 2001.